Microenvironment pH-Induced Selective Cell Death for Potential Cancer Therapy Using Nanofibrous Self-Assembly of a Peptide Amphiphile

Yamamoto, Shota ; Nishimura, Kanon ; Morita, Kenta ; Kanemitsu, Sayuki ; Nishida, Yuki ; Morimoto, Tomoyuki ; Aoi, Takashi ; Tamura, Atsuo ;…

(Citation)
Biomacromolecules,22(6):2524-2531

(Issue Date)
2021-06-14

(Resource Type)
journal article

(Version)
Accepted Manuscript

Microenvironment pH-induced selective cell death for potential cancer therapy using nanofibrous self-assembly of a peptide amphiphile

Shota Yamamoto,[a] Kanon Nishimura, [a] Kenta Morita, [a] Sayuki Kanemitsu, [a] Yuki Nishida,[a] Tomoyuki Morimoto, [a] Takashi Aoi[b], Atsuo Tamura[c] and Tatsuo Maruyama[a, d]*

[a]Department of Chemical Science and Engineering, Graduate School of Engineering, Kobe University, 1-1 Rokkodai, Nada-ku, Kobe 657-8501, Japan.

[b]Division of Advanced Medical Science, Graduate School of Science, Technology and Innovation, Kobe University, Kobe 657-8501, Japan.

[c]Graduate School of Science, Department of Chemistry, Kobe University, Nada, Kobe 657-8501, Japan.

[d]Research Center for Membrane and Film Technology, Kobe University, 1-1 Rokkodai, Nada, Kobe 657-8501, Japan

KEYWORDS. antitumor, cytotoxicity, lipopeptide, nanofiber, pH-sensitive

Abstract

Self-assembly of synthetic molecules has been drawing a broad attention as a novel emerging approach in drug discovery. Here we report selective cell death induced by a novel peptide amphiphile that self-assembles to form entangled nanofibers (hydrogel) based on intracellular pH (pH_i). We found that a palmitoylated hexapeptide (C_{16}-VVAEEE) formed a hydrogel below pH 7. The formation of the nanofibrous self-assembly was responsive to a small pH change around pH 7. The cytotoxicity of C_{16}-VVAEEE was correlated with pH_i of cells. Microscope observation demonstrated the self-assembly of C_{16}-VVAEEE inside HEK293 cells. In vivo experiments revealed that the transcutaneous administration of C_{16}-VVAEEE showed remarkable anti-tumor activity. This study proposes that distinct microenvironment inside living cells can be used as a trigger for the intracellular self-assembly of a peptide amphiphile, which provide a new clue to drug discovery.

Introduction

Molecular self-assembly is a powerful bottom-up strategy to create higher order structures from nanoscales to microscales. It produces a wide range of intelligent materials integrating various functional properties.[1-2] The molecular self-assembly works as "molecular ensemble" to show attractive features for drug delivery, biosensing, chemical reactions and well-designed nanostructures, which are not achieved by monomeric molecules.[3-5] In the last two decades, a number of studies reported the self-assembly of peptide amphiphiles (PAs or lipopeptides) and amino-acids amphiphiles. As amino acids are a basic building block of proteins to create fascinating functions in nature, a PA with an appropriate molecular design has a high potential to realize protein-mimic functions.[6] Indeed, there are many reports describing that the self-assemblies of PAs work as cell scaffolds, catalysts, analytical device, drug carriers, pharmacologically active materials, pollutant adsorbents, emulsion stabilizer etc.[7-13]

Among the proposed applications of PAs, pharmacological activity of the self-assembly of PAs has brought a novel approach with a high impact to the field of drug discovery, which is totally different from conventional concepts of drugs (small molecule drugs, inhibitors and antibody drugs).[14] Xu and coworkers first demonstrated that PAs killed animal cells and bacteria via enzyme-instructed intracellular self-assembly.[15-16] Their studies showed the remarkable cytotoxicity of their PAs while there are a variety of natural and synthetic PAs with low or negligible cytotoxicity.[17-20] To deliver the PAs inside cells, Xu et al employed their precursors (phosphorylated peptides) to prevent the self-assembly of PAs outside cells. Dephosphorylation inside cells, which was catalyzed by overexpressed phosphatase, converted the precursors to PAs to allow the intracellular self-assembly, leading to cell death.[14-16, 21] Inspired from their studies, we succeeded in the selective death of cancer cells induced by the intracellular self-assembly of a PA, in which cancer-related proteinase

promoted the cell uptake of the PA and its intracellular self-assembly.[22] Other groups also reported the fate control of cancer cells via the intracellular self-assembly of PAs.[23-25]

Above studies employed enzymes, which were overexpressed in diseased cells, to trigger the intracellular self-assembly. In addition to overexpression of enzymes, there are variations in physiological conditions of diseased cells and tissues that are different from those of normal ones.[26-28] For example, abnormal levels of reactive oxygen species and nitric oxide inside cells are related with various diseases[29-30] and malfunction of a living system causes pH change inside and outside the cells.[26, 28, 31] Tumor pH (extracellular pH) was less than pH 7.1, while that of normal cells is around pH 7.4.[28, 32] Intercellular pH of some tumor spheroids is slightly acidic (below pH 7).[33-34] Some of viral and bacterial infections decrease intracellular pH (pH_i) slightly.[26, 31, 35]

Although there are many studies employing abnormal extracellular pH as a trigger to control drug release around targeted cells or parts of a body,[36-42] there is, to our knowledge, no report on the pharmacological activity of the molecular self-assembly triggered by pH_i of diseased cells. In the present study, we designed a novel PA that self-assemble by a small pH change around neutral pH to form entangled nanofibers (Figure 1). We succeeded in the self-assembly of the PA inside the cells triggered by the slightly low pH_i, which induced the selective death of cells with slightly low pH_i. In vivo experiments revealed that the transcutaneous administration of the PA inhibited the tumor growth and reduced the tumor size on mice. The present study demonstrates that an appropriate molecular design of a PA leads to the high pH sensitivity of its self-assembly. The self-assembly of the PA, which is highly sensitive to microenvironment pH in a living body, offers a new approach for selective removal of cells[43] and drug discovery.

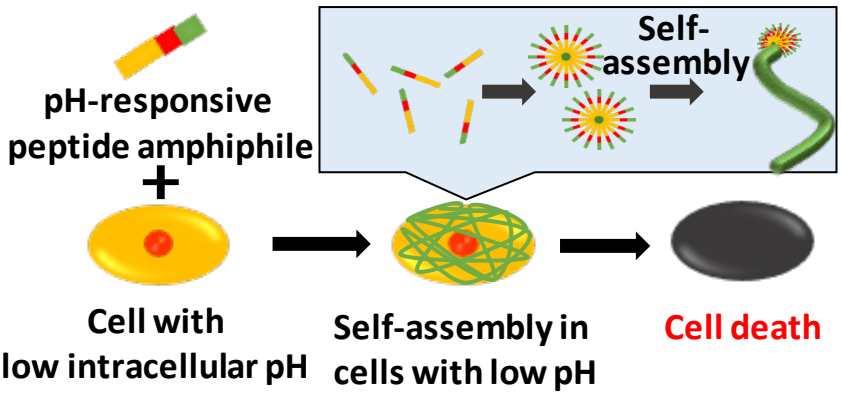

Figure 1. Schematic illustration of selective cell death induced by molecular self-assembly of intracellular pH-responsive peptide amphiphile (PA).

Experimental

Solid-phase syntheses of peptide amphiphile. Peptide amphiphiles (C_{16}-VVAEEE, C_{10}-VVAEEE and C_8-VVAEEE) were synthesized by standard 9-fluorenylmethoxycarbonyl (Fmoc) solid-phase peptide synthesis on a 0.6-mmol scale. H-Glu(OtBu)-(Trt)-Trt(2-Cl)-resin was used as the polymeric support. Fmoc-Glu(OtBu)-OH (3 equiv.) was coupled to the resin (0.6 mmol) using HBTU and HOBT·H_2O as coupling agents in the presence of DIEA in DMF for 60 min at room temperature. Palmitic acid (3 equiv.) was coupled to the N-terminus of the synthesized peptide using the coupling agents in the presence of DIEA in DMF for 90 min at room temperature. After each coupling reaction, the Fmoc groups were removed by mixing with a piperidine/DMF (20/80) mixture for 45 min at room temperature. Cleavage of the synthesized peptides from the resin was performed in a mixture of TFA, TIPS and water at a volume ratio of 95:2.5:2.5 for 90 min at room temperature. The synthesized peptides in the cleavage mixture were precipitated with 0.1 M hydrochloric acid, collected by centrifugation, washed three times with 0.1 M hydrochloric acid and freeze-dried. The crude peptides were purified using a high-performance liquid chromatography (HPLC) system (LC-20AT, Shimadzu, Kyoto, Japan) equipped with an Inertsil ODS-3 column (10 × 250 mm, GL Science,

Tokyo, Japan). The purified product was freeze-dried and obtained as a dry white powder in 42% yield. The obtained product was identified by matrix-assisted laser desorption ionization time-of-flight mass spectrometry (MALDI-TOF/MS) using an UltrafleXtreme TM mass spectrometer (Bruker, Billerica, MA, USA). MALDI-TOF/MS (SA matrix) (*m/z*): $[M+K]^+$ calcd for C_{16}-VVAEEE ($C_{44}H_{76}N_6O_{14}$), 951.51; found, 952.56 (Supporting Information Figure S1). $[M+Na]^+$ calcd for C_{10}-VVAEEE ($C_{38}H_{64}N_6O_{14}Na$), 851.43; found, 851.49 (Figure S2). $[M+Na]^+$ calcd for C_8-VVAEEE ($C_{36}H_{60}N_6O_{14}Na$), 823.40; found, 823.49 (Figure S3).

Solid-phase syntheses of NBD-C_{12}-VVAEEE. Condensation of amino acids and Fmoc-Adod(12)-OH were carried out by the same protocol as described above. To conjugate NBD-Cl with a N terminus of NH_2-C_{12}-VVAEEE-resin, 1.8 mmol NBD-Cl, 680 μL DIEA, 7.72 mL DMF were added to the column and reacted for 24 h in a dark. Cleavage of the synthesized peptides from the resin and purification of the peptide were the same as described above. The obtained product was identified by matrix-assisted laser desorption ionization time-of-flight mass spectrometry(*m/z*): $[M+H]^+$ calcd for $C_{46}H_{70}N_{10}O_{17}Na$, 1057.48; found, 1057.68 (Figure S4).

Gelation tests. Gelator (0.15 wt%) in phosphate buffered saline without Ca^{2+} and Mg^{2+} (PBS) (pH 7.4, 50 mM, 100 μL) was added to a glass tube (diameter: 8 mm) containing a peptide amphiphile (0.15 wt%) in phosphate buffer solution (pH 7.4, 50 mM, 1.0 mL). After it was mixed well at 85 °C for 10 min, the solution was kept for 24 h at room temperature without stirring. After 24 h, gelation was confirmed by inversion of the glass tube containing the solution.

TEM observation. Transition electron microscopy (TEM) measurements were carried out

using a transmission electron microscope (JEOL2100F, JEOL, Tokyo, Japan). A piece of gel (0.15 wt%) was placed on a carbon-coated copper grid and stained with phosphotungstic acid (1 wt%). The grid was dried overnight under vacuum and observed using an acceleration voltage of 200 kV.

CD spectrum measurement. CD spectrum measurement was performed at 25 °C on a Jasco J-725K CD instrument using 10 mm quartz cuvettes. The concentration of the samples was 0.15 wt% in PBS.

Critical micellar concentration (CMC) measurements. C_{16}-VVAEEE solutions of varied concentration were prepared in PBS buffer at pH 6.8 and pH 7.4. Rhodamine 6G was added to the C_{16}-VVAEEE solutions to give a final rhodamine 6G concentration of 5 μM. λmax was determined by measuring the absorbance from 520 to 540 nm using a fluorescence spectrophotometer (FP-8200, Jasco, Tokyo, Japan).

Culture of cells. Frozen cells were harvested by rapid thawing in a 37°C water bath and were washed with fresh medium (DMEM with 10 % fetal bovine serum and 1 % penicillin/streptomycin or Complete Medium Kit with serum and CultureBoost-R™ (Cell Systems)). The medium was exchanged 2 times a week. Cultures of cells were maintained at 37°C and 5% CO_2.

Intracellular pH measurement. Intracellular pH was measured using pHrodo™ Green AM Intracellular pH Indicator purchased from Thermo Fisher Scientific Inc. and a flow cytometer (BD Facscanto II, Becton, Dickinson and Company, NJ) according to the manufacturer's instruction.

***In vitro* cell viability.** Cytotoxicity of the peptide amphiphiles was evaluated using Cell Count Reagent SF (Nacalai tesque, Kyoto, Japan) in accordance with the manufacturer's instructions, which is a modified version of the MTT assay using a highly water-soluble tetrazolium salt. Briefly, cells were plated at a seeding density of 2.0×10^4 cells/well in 96-well plates and incubated for 24 h. Then, a fresh medium containing a peptide amphiphile at a given concentration was added to each well. The cells were typically exposed to a peptide amphiphile for 24 h and with given concentrations, and then treated with a 10 μL solution of Cell Counting Kit-8. After incubation for 1 h, the absorbance at 450 nm of each well was measured using a microplate reader (SH9000, Hitachi igh-Technologies Corporation, Tokyo, Japan).

Live/dead assay. The survival of cells exposed to the peptide amphiphile medium solution was evaluated using a LIVE/DEAD Viability/Cytotoxicity kit (Molecular Probes, Invitrogen, Carlsbad, CA). Samples were processed according to the manufacturer's instruction. Briefly, after allowing the cells to adhere to a dish surface, 1.0×10^5 cells/well in a glass-base dish were incubated with and without a peptide amphiphile at 37 °C for 24 h. Cells were stained with the LIVE/DEAD assay reagents and then incubated at 37 °C for 20 min. After washing with warm 1 mL Living Cell Imaging Solution, cells were then observed using a confocal laser scanning microscope (CLSM) (Fluoview FL1000, Olympus, Tokyo, Japan). Live cells were stained with green fluorescence and dead cells were with red fluorescence.

Visualization of cellular uptake using NBD-C_{12}-VVAEEE. 1.0×10^5 cells/well in a glass-base dish were incubated with and without a peptide amphiphile at 37°C for 24 h. 0.3 wt% C_{16}-VVAEEE in PBS and a 0.15 wt% NBD-C_{12}-VVAEEE in D-PBS were diluted 10 times and 1000 times with the culture medium, respectively. Their final concentrations were 0.03 wt%

and 1.5×10^{-4} wt%. The medium in the dish was replaced with the medium containing the peptide amphiphiles and incubated in CO_2 incubator for 24 h. The medium in the dish was replaced with LCIS containing Hoechst (1000-fold dilution) and incubated for 15 min. After washing with warm LCIS, cells were observed using a CLSM.

Visualization of NBD-C_{12}-VVAEEE accumulated at ER. HEK293 cells, which were incubated with 0.05 wt% C_{16}-VVAEEE in PBS and a 5×10^{-3} wt% NBD-C_{12}-VVAEEE for 24 h in a glass-base dish, were treated for 30 min at 37 °C with a fluorescent ER-Tracker™ Red (E34250, ThermoFisher, Waltham, MA) to stain ER according to the manufacturer's protocols. The staining solution was replaced with a fresh DMEM, followed by CLSM observation.

Spheroid preparation. Spheroids of HEK293 and A431 cells were prepared in a U-shaped 96-hole microplate (MS-9096U, Sumitomo Bakelite Co., Ltd., Tokyo, Japan). Cells (5.0×10^3) suspended in a 200 μL DMEM were placed in a well of a U-shaped microplate, followed by incubation in DMEM medium for 4 d. The supernatant was replaced with fresh DMEM medium containing C_{16}-VVAEEE at given concentrations. After 24 h, the spheroids were stained with the LIVE/DEAD Viability/Cytotoxicity kit and observed by CLSM.

Apoptotic/necrotic assay. Apoptotic/necrotic/healthy cells detection kit (Promo cell, GmbH, Heidelberg, Germany) was used to detect the apoptosis according to the manufacturer's protocols. Briefly, HeLa cells in a glass-base dish were washed with a binding buffer. A staining solution was added to microplate wells and cells were incubated for 15 min at 25 °C, followed by washing with a binding buffer. Cells were visualized using a CLSM.

Preparation of solid-in-oil dispersion containing PA. An aqueous solution containing PA

and octaarginine (R8) (0.5 mg/mL each) and a cyclohexane solution containing 12.5 mg/mL sucrose laurate (L-195, Mitsubishi-Kagaku Foods, Tokyo, Japan) were mixed at a 1:2 (v:v) ratio and homogenized using a homogenizer (PRO200, PRO Scientific Inc., Oxford, CT) at 35000 rpm for 2 min. The water-in-oil emulsion prepared was frozen in liquid nitrogen and freeze-dried for 24 h to yield a PA/R8−L195 complex as a white solid. The complex was dispersed in isopropyl myristate (IPM) to give the complex dispersion at 1.5 wt% PA in IPM (PA-solid-in-oil dispersion, abbreviated PA-S/O dispersion).

The PA-S/O dispersion (200 μl) was put on an adhesive tape (Band-aid Water-Block, Johnson & Johnson, New Brunswick, NJ) (abbreviated PA-S/O patch).

In vivo experiments. Female BALB/c nude mice (5 weeks old) were purchased from Japan SLC (Shizuoka, Japan) and maintained under standard conditions for 1 week. All animal experiments were carried out at Japan SLC in accordance with the institutional guideline for the care and use of laboratory animals (approval no. F71-8128).

BALB/c nude mice bearing HeLa tumor tissues were prepared by subcutaneously injecting 100 μL of a suspension of HeLa S cells (1×10^7 cells) into the flank. On day 14 after the inoculation, the mice were randomly assigned to 4 groups (n = 7): (i) no treatment (control), (ii) S/O dispersion without a patch (iii) PA-S/O dispersion without a patch and (iv) PA-S/O patch. The dispersions were applied to the areas of tumor and the application was repeated using fresh ones 3 times a week. Patches were placed on the areas of tumor and replaced with fresh ones 3 times a week. Tumor sizes were measured 3 times a week using a caliper, and the tumor volumes were calculated using the following formula:

$$\text{Tumor volume } (mm^3) = \text{longer diameter} \times \text{shorter diameter}^2 \times 0.5$$

Mice were sacrificed when the tumor volume exceeded 2000 mm^3. The statistical significance of differences in anti-tumor efficacy between two groups possessing unequal

variance was evaluated using the Tukey test. Differences were considered significant at a 95% confidence level ($p < 0.05$).

Results and discussion

Synthesis and characterization of a pH-responsive peptide amphiphile (C_{16}-VVAEEE).

To find the peptide amphiphile that exhibited sol-gel transition responsive to a small pH change around neutral pH, we designed and synthesized 9 different kinds of peptide amphiphiles by solid-phase peptide synthesis. The peptide sequences of the synthesized PAs were designed to have hydrophobic amino acid residues and acidic amino acid residues for pH-responsive self-assembly.[44-49] We then carried out gelation tests using Dulbecco's phosphate buffered saline (PBS) (Table S1). Among the various synthesized peptide amphiphiles, 0.15 wt% C_{16}-VVAEEE (*N*-palmitoyl-Val-Val-Ala-Glu-Glu-Glu, Figure 2a) exhibited hydrogel formation, which was very sensitive to a small pH change around pH 7. It formed transparent hydrogel at pH 6.8 (Figure 2b), while it did not above pH 7.0 (Figure 2b). C_{16}-VVAEEE was composed of 3 parts: (1) a C16 alkyl chain to enhance self-assembling ability by hydrophobic interaction,[44, 50] (2) a tripeptide segment (Val-Val-Ala) following the alkyl chain to create β-sheet by hydrogen bonding.[51-52] (3) the peptide sequence (Glu-Glu-Glu) that acts as a pH-responsive part due to the carboxyl groups of the side chains and the C-terminus.[48] The hydrogel of C_{16}-VVAEEE exhibited reversible sol-gel transition by heating/cooling and also by controlling pH. It should be noted that C_{16}-VVAEEE keeps hydrogel over a wide range of acidic pH (e,g. pH 4 and pH 5).

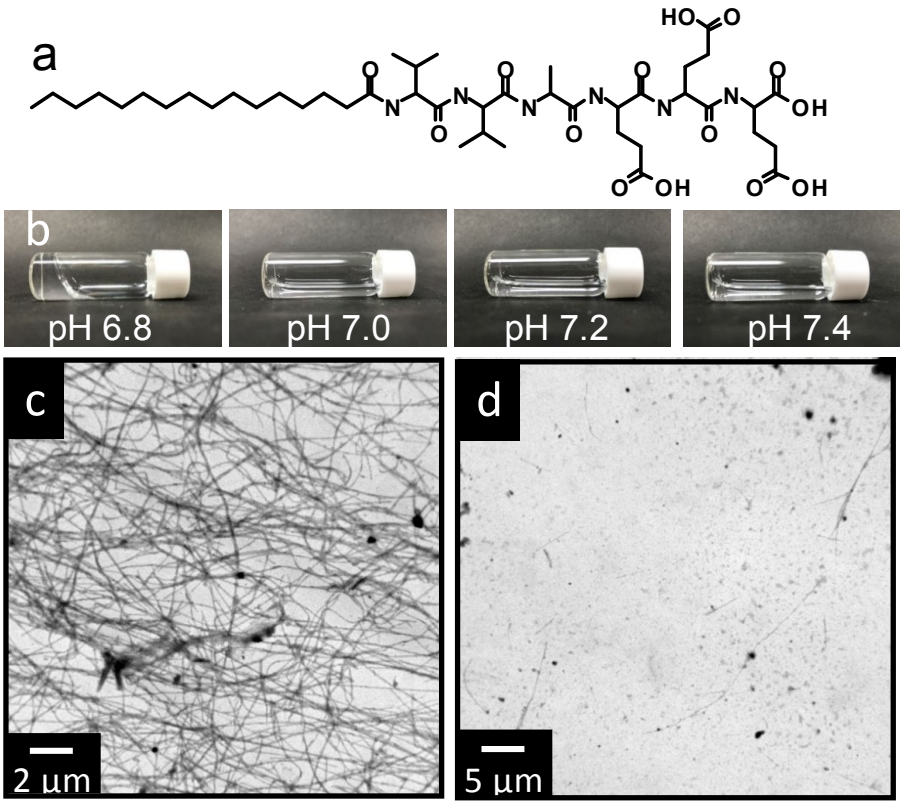

Figure 2 (a) Molecular structure of *N*-palmitoyl-Val-Val-Ala-Glu-Glu-Glu (C_{16}-VVAEEE). (b) Gelation tests of PBS after 24 h at various pH. The concentration of C_{16}-VVAEEE was 0.15 wt%. (c, d) TEM images of the freeze-dried hydrogel and PBS solution of 0.15 wt% C_{16}-VVAEEE. (c) pH 6.8, (d) pH 7.4.

Transmission electron microscope (TEM) observation revealed branched or entangled long nanofibers with a diameter of a few tens of nanometres in the hydrogel of C_{16}-VVAEEE at pH 6.8 (Figure 2c & d). There observed only a few short nanofibers (less than 30 μm in length), which were not connected each other, in the solution at pH 7.4. These results suggested that C_{16}-VVAEEE self-assembled to form long entangled nanofibers at pH 6.8, and that nanofiber formation were involved in the gelation.

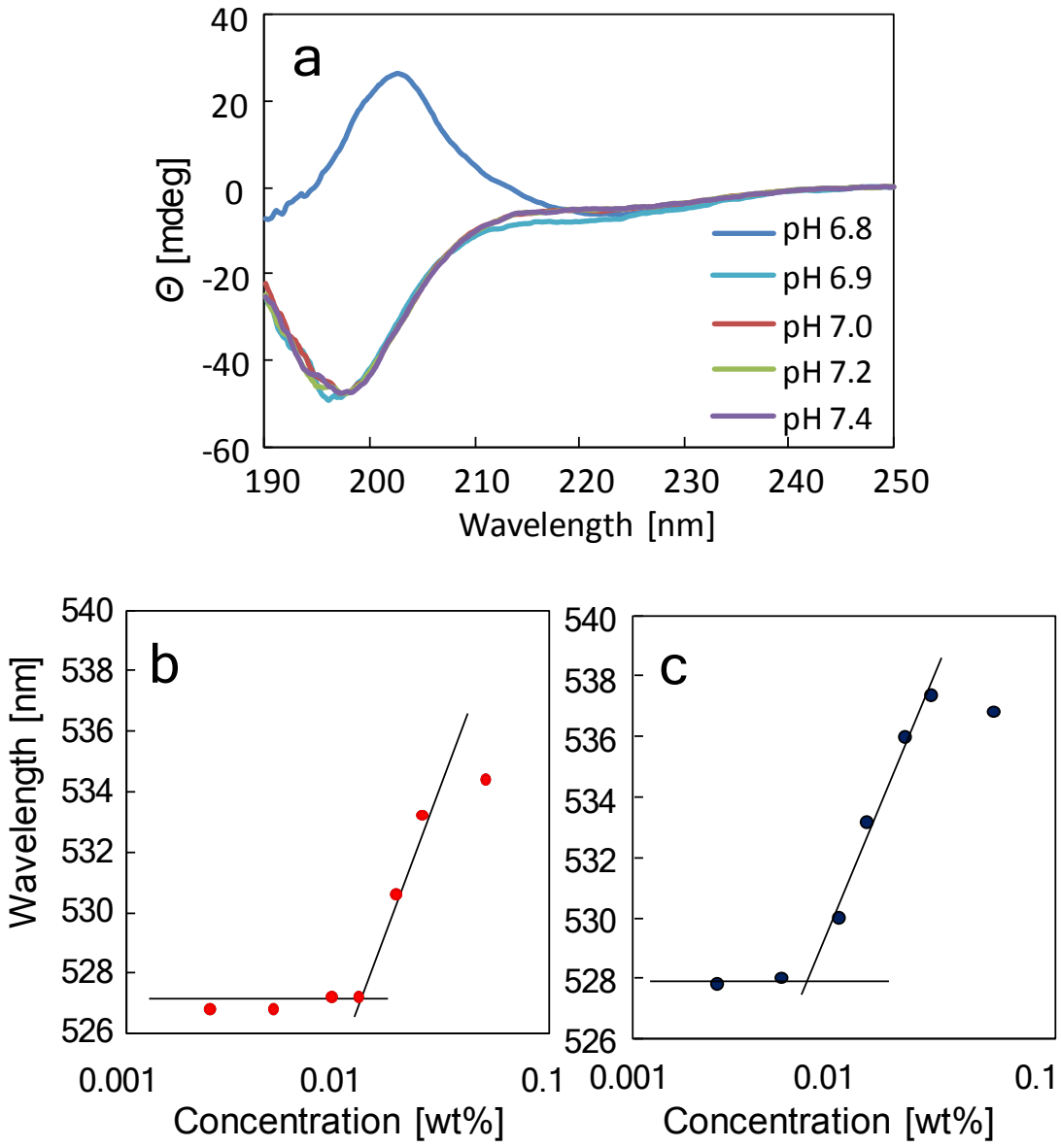

Figure 3 a) CD spectra of C_{16}-VVAEEE aqueous solution (0.05 wt%) at various pH. (b, c) Measurements of critical micellar concentrations (CMC) using rhodamine 6G for C_{16}-VVAEEE in PBS. (b) pH 6.8 (c) pH 7.4.

To evaluate the self-assembled structure of C_{16}-VVAEEE in aqueous solution, CD spectra of the solutions were measured at varied pH (Figure 3a). A positive peak was observed around 203 nm at pH 6.8, which was considered to be derived from a β-sheet structure.[48] On the other hand, negative peaks were observed around 198 nm at pH 6.9-7.4, which was considered to be

derived from a random-coil structure. The CD spectra showed that the supramolecular structure of C_{16}-VVAEEE in aqueous solution greatly changes according to a small pH change from pH 6.9 to pH 6.8.

The critical micellar concentration (CMC) of C_{16}-VVAEEE was evaluated using rhodamine 6G in PBS.[53] The CMC depended on pH (Figure 3b and c). The CMCs at pH 6.8 and pH 7.4 were 2.3×10^{-3} wt% and 1.1×10^{-2} wt%, respectively. The CMC measurements indicated that a small variation in the pH environment drastically affected the monomeric solubility of C_{16}-VVAEEE and also altered the intermolecular interaction of C_{16}-VVAEEE. These results meant that a slightly acidic condition (~pH 6.8) triggered the self-assembly of C_{16}-VVAEEE. Although the p*K*a of carboxy groups in a side chain and in a C-terminus of Glu were 4.3 and 2.2, the critical pH value for the self-assembly of C_{16}-VVAEEE was ~pH 6.8. There is a report that neighboring carboxy groups in a protein molecule affect each other and greatly increase the p*K*a.[54] The continuum of three Glu residues and the self-assembly of C_{16}-VVAEEE would contribute to the p*K*a shift in the present study. Indeed, Goldberger and co-workers also reported the dynamic morphological change of the self-assembly of the Glu-rich PA in response to a pH change at pH 6.6.[48-49]

Intracellular pH and cytotoxicity of C16-VVAEEE to various kinds of human cells.

We measured the pH_i of four different kinds of human cell lines (MvE, A431, HeLa and HEK293 cells) cultured on microplates. MvE cells are non-cancer cells derived from primary normal human dermal microvascular endothelial cells. A431 and HeLa cells are the cell lines derived from an epidermoid carcinoma and cervical cancer cells. HEK293 cells are the immortalized cell line derived from human embryonic kidney cells, which proliferate indefinitely. pHrodo ™ Green AM Intracellular pH Indicator was used to measure cytoplasm pH of cells cultured on a dish. The pH_i values of these cells are summarized in Figure 4a. The

pH_i of HEK293 and HeLa cells were 6.7 and 7.1, respectively, which were slightly lower than those of A431 and MvE cells (pH 7.5). HeLa cells are derived from cells infected with human papillomavirus, which may explain the difference in the pH_i when compared with that of other cancer cells.

a

Cell line	intracellular pH (pH_i)
MvE	7.5
A431	7.5
HeLa	7.1
HEK293	6.7

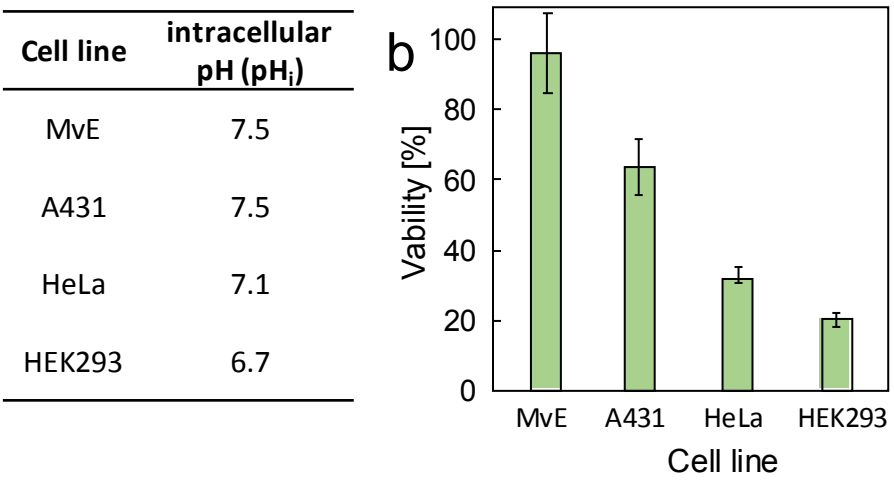

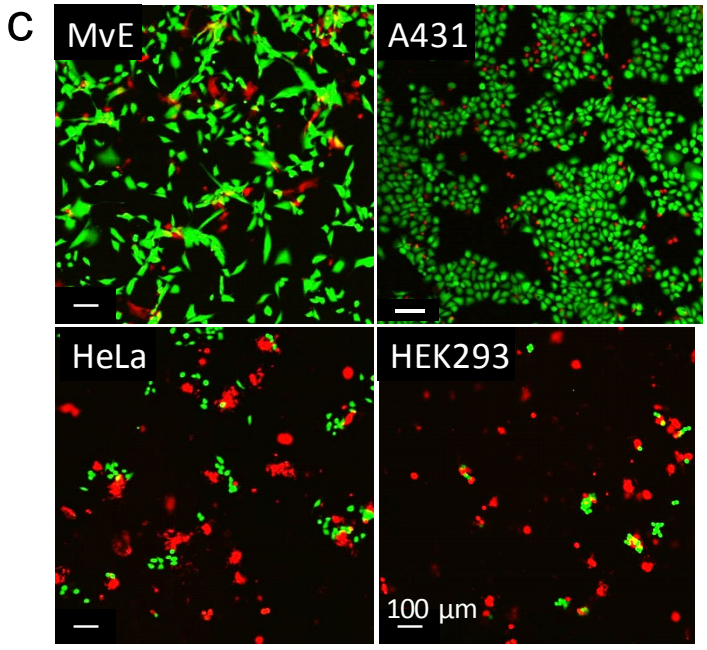

Figure 4. a) Measurement of the intracellular pH (pH_i) of four different cell lines using the pHrodo™ Green AM Intracellular pH Indicator. b) Viability assay of the four different kinds of human cell lines after incubation with C_{16}-VVAEEE (0.05 wt%) for 24 h. c) Live/dead assays of the four different kinds of human cell lines after incubation with C_{16}-VVAEEE (0.05 wt%)

for 24 h. Cells cultured on the 96-well microplates were observed using a confocal laser scanning microscope (CLSM). Green and red fluorescence means living and dead cells, respectively.

The cytotoxicity of C_{16}-VVAEEE (0.05 wt%) was evaluated using the four different kinds of human cell lines. Cell viability was quantified using Cell Count Reagent SF (Nacalai tesque, Kyoto, Japan), which is a modified version of the MTT assay using a highly water-soluble tetrazolium salt. C_{16}-VVAEEE was added in culture medium and it looked "dissolved" prior to the cytotoxicity tests. Figure 4b showed that C_{16}-VVAEEE was highly toxic to HEK293 cells and also toxic to HeLa cells, of which pH_i was relatively low. C_{16}-VVAEEE exhibited negligible or low cytotoxicity to MvE and A431 cells, of which pH_i was 7.5. The live/dead assay using CLSM also demonstrated that there were relatively a small number of HeLa and HEK293 cells on microplates and many of them were dead (red fluorescence) (Figure 4c). On the other hand, a number of MvE and A431 cells were observed and most of them were alive (green fluorescence). C_{16}-VVAEEE exhibited remarkable cytotoxicity to the cells with low pH_i (pH 6.8 and 7.1) and not to the cells of pH 7.5.

The effect of the C_{16}-VVAEEE concentration was also examined (Figure S5). The C_{16}-VVAEEE concentration did not affect the viability of MvE cells over the range of the tested concentration. The viability of A431 cells were slightly affected by the C_{16}-VVAEEE concentration. The viability of HEK293 and HeLa cells remarkably decreased with the increase of the C_{16}-VVAEEE concentration.

Visualization of cell uptake of a PA

To verify the cell uptake of a peptide amphiphile and self-assembly inside cells, HEK293 cells were incubated with C_{16}-VVAEEE, NBD-C_{12}-VVAEEE and ER-Tracker (red

fluorescence). NBD-C_{12}-VVAEEE was an analogue of C_{16}-VVAEEE and had a fluorophore (7-nitrobenzo-2-oxa-1,3-diazole, NBD) at the end of its alkyl chain (Figure 5a). We already confirmed that C_{16}-VVAEEE and NBD-C_{12}-VVAEEE formed nanofibers via co-assembly due to the structural homology. Since NBD is a green fluorophore that is sensitive to hydrophobic environment, it serves as a probe for intracellular fiber formation of PAs.[24, 55] The CLSM observation (Figure 5b) revealed green fluorescence, indicating that C_{16}-VVAEEE was taken by HEK293 cells and suggested that the self-assembly of C_{16}-VVAEEE and NBD-C_{12}-VVAEEE inside the cells.

Figure 5b (Merge) shows there are overlaps of green and red fluorescence in many areas, suggesting the accumulation of C_{16}-VVAEEE at endoplasmic reticulum (ER). To discuss the mechanism of cell death, we carried out apoptosis/necrosis assay. Figure S6 shows green fluorescence (FITC-annexin V) on HEK293 cells after incubation with C_{16}-VVAEEE for 3 h. A little portion of red fluorescence (propidium iodide) was observed. These observation suggested that HEK293 cells incubated with C_{16}-VVAEEE were in early apoptosis.[56] Since ER stress often induces apoptosis,[57] the accumulation of the self-assembly of C_{16}-VVAEEE at ER would also induce apoptotic death of HEK293 cells in the present study. Indeed, some groups reported anti-cancer activity induced by targeted ER stress.[58-60]

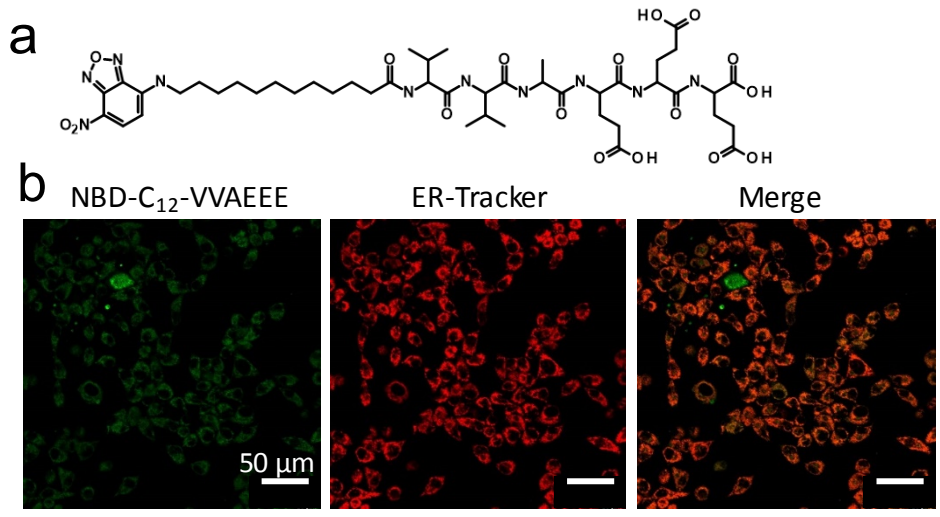

Figure 5 a) Molecular structure of NBD-C_{12}-VVAEEE. b) CLSM images of HEK293 cells

stained with ER-tracker after incubation with a mixture of C_{16}-VVAEEE (0.05 wt%) and NBD-C_{12}-VVAEEE (5.0×10^{-4} wt%).

Molecular design of peptide amphiphiles for the cytotoxicity

One of the key factors for the self-assembly is the hydrophobic moiety of the PA.[61] We then synthesized another two different kinds of PAs (Figure 6a). These PAs had C8 and C10 as alkyl chains to reduce the self-assembling ability. The viability assay demonstrated that C_8-VVAEEE and C_{10}-VVAEEE exhibited negligible or low cytotoxicity to the four different kinds of cells (Figure 6b). The cytotoxicity of the PA decreased with the decrease of the alkyl-chain length. These results indicated two possibilities. One is the effect of the self-assembling ability of PAs on the cytotoxicity[22, 62] and the other is interaction of an acyl chain with an organelle or a membrane that might localize PAs at specific positions inside cells.[63]

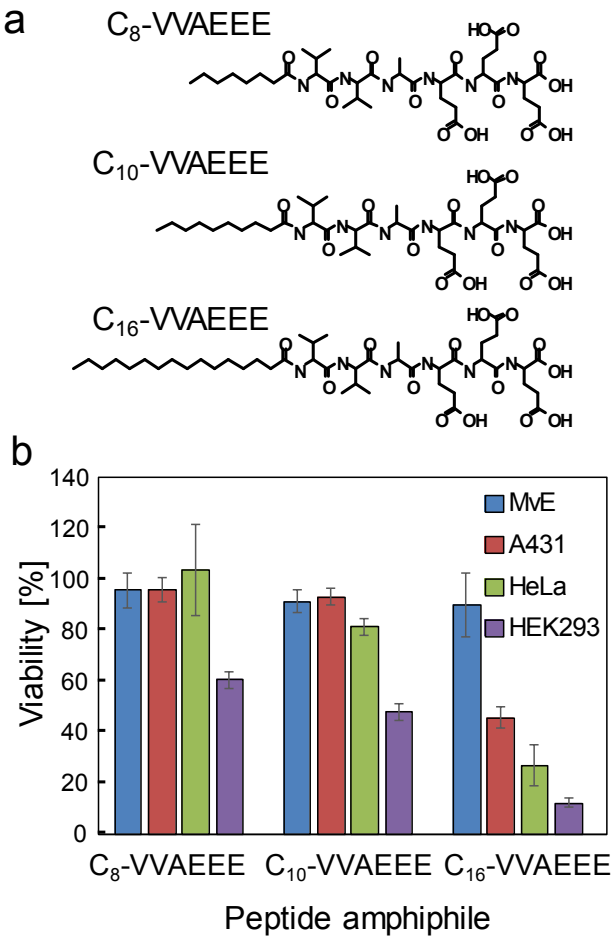

Figure 6 a) Molecular structures of PAs with alkyl chains of different lengths. b) Viability assay of different cell lines after incubation with PAs (0.05 wt%) for 24 h.

Live/dead assay for spheroids treated with C_{16}-VVAEEE

A spheroid of cells is a simple form of three-dimensional cell culture. We prepared spheroids of HEK293 and A431 cells and investigated the cytotoxicity of C_{16}-VVAEEE to the spheroids. Figure 7a showed that there were many dead cells in the core of the spheroid of HEK293 cells when it was treated with 0.015 wt% C_{16}-VVAEEE. At a low concentration of C_{16}-VVAEEE (0.005wt%), there observed a few number of dead cells and living cells forming the rim of the spheroid. On the other hand, the spheroid of A431 cells kept alive at the tested concentrations of C_{16}-VVAEEE.

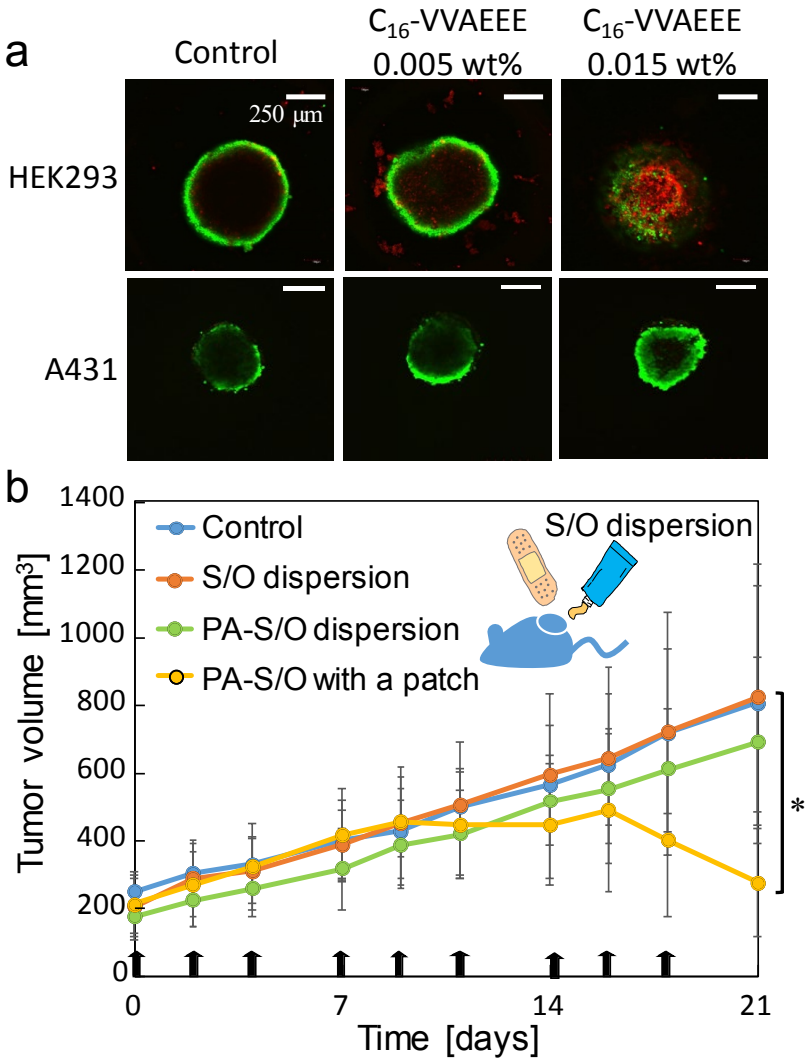

Figure 7. a) CLSM observation for Live/dead assay of spheroids (HEK293 cells and A431 cells) incubated with C_{16}-VVAEEE for 24 h. b) Tumor growth in HeLa tumor-bearing mice. Arrows indicate the administration of the S/O dispersion. Error bars represent the standard deviations of 6 mice per group. Control means tumor-bearing mice without any treatment. n = 8. *$p < 0.05$.

In vivo tumor growth inhibition

Finally, we evaluated the antitumor activity of C_{16}-VVAEEE in vivo. Nude mice subcutaneously xenografted with HeLa tumors were prepared. To administer the PA, we

adopted a solid-in-oil (S/O) dispersion system for the transcutaneous delivery of the PA.[64-65] A S/O dispersion is an oil-based dispersion containing lyophilized particles of hydrophilic molecules/surfactants complexes. We prepared a PA/edible surfactant complex and dispersed the complex in isopropyl myristate (IPM) at 0.15wt% PA (PA-S/O dispersion) according to Goto's procedure.[65] The fresh S/O dispersion was put on a tumor site of a mouse 3 times a week. Since the S/O dispersion was fluid, administration with a patch was also investigated. Figure 7b shows the tumor growth on mice during the transcutaneous administration of the PA. Although there was no obvious difference in the first week, the tumor growth on mice with the PA/patch was inhibited from the 2nd week and the tumor size decreased from day 15. The photos of mice after the administration for 3 weeks also exhibit the obvious difference in the tumor size (Figure S7). The S/O dispersion without the PA and the PA-S/O dispersion without a patch did not inhibit the tumor growth. A patch would keep the fluid dispersion on a tumor site and help the transcutaneous delivery. These results demonstrate anti-tumor activity of C_{16}-VVAEEE in vivo and the transcutaneous delivery of the PA that works for tumor reduction.

Conclusion

In the present study, we synthesized a novel PA (C_{16}-VVAEEE), of which self-assembly was highly responsive to a small pH change around neutral pH. C_{16}-VVAEEE self-assembled to form entangled nanofibers, leading to hydrogelation below pH 7. A long alkyl chain and hydrophobic amino acids (Val and Ala) residues contributed to the self-assembly. The continuum of Glu created the pH-sensitivity of the PA around pH 7, which was far from p*K*a of the carboxy group in the side chain of Glu. The PA exhibited cell-selective cytotoxicity according to pH_i. The cells with low pH_i were killed by the PA. Various investigations indicated that the intracellular self-assembly of the PA played an important role for the selective cell death and also that the self-assembly was induced by low pH_i. The present study reveals that

microenvironment pH inside cells can be used as a trigger for the intracellular self-assembly of a PA, which allows us to control the cell fate in a cell-selective manner. In vivo experiments demonstrate that the transcutaneous delivery of the PA exhibited the anti-tumor activity and reduced the tumor size (not only inhibiting the tumor growth). The self-assembly of a PA is tunable for various kinds of stimuli by designing the chemical structure of a PA. This will extend the potential of a PA as a highly cell-selective drug or a cell-selection tool for diseased cells and pathogenic microorganisms.

ASSOCIATED CONTENT

Supporting Information. Materials and Supplementary Results (PDF). This material is available free of charge via the Internet at http://pubs.acs.org.

AUTHOR INFORMATION

Corresponding Author

tmarutcm@crystal.kobe-u.ac.jp

ORCID

Tatsuo Maruyama: 0000-0003-2428-1911

Author Contributions

The manuscript was written through contributions of all authors. All authors have given approval to the final version of the manuscript.

Funding Sources

This study was financially supported by Takeda Science Foundation, The Uehara Memorial Foundation, and by JSPS KAKENHI Grant 20H02542, 20H04711 and 19H05458.

Notes

The authors declare no competing financial interest.

ACKNOWLEDGMENT

The authors thank Prof. A. Kondo for his technical help with MALDI-TOF/MS.

ABBREVIATIONS

pH_i, intracellular pH; MvE cells, non-cancer cells derived from primary normal human dermal microvascular endothelial cells; A431 cells, an epidermoid carcinoma; HeLa cells, cervical cancer cells; HEK293 cells, an immortalized cell line derived from human embryonic kidney cells.

References

(1) Ulijn, R. V.; Smith, A. M., Designing peptide based nanomaterials. *Chem. Soc. Rev.* **2008,** *37* (4), 664-75.
(2) Cui, H.; Webber, M. J.; Stupp, S. I., Self-assembly of peptide amphiphiles: from molecules to nanostructures to biomaterials. *Biopolymers* **2010,** *94* (1), 1-18.
(3) Aida, T.; Meijer, E. W.; Stupp, S. I., Functional supramolecular polymers. *Science* **2012,** *335* (6070), 813-7.
(4) Shigemitsu, H.; Hamachi, I., Design Strategies of Stimuli-Responsive Supramolecular Hydrogels Relying on Structural Analyses and Cell-Mimicking Approaches. *Acc. Chem. Res.* **2017,** *50* (4), 740-750.
(5) Trausel, F.; Versluis, F.; Maity, C.; Poolman, J. M.; Lovrak, M.; van Esch, J. H.; Eelkema, R., Catalysis of Supramolecular Hydrogelation. *Acc. Chem. Res.* **2016,** *49* (7), 1440-1447.
(6) Singh, N.; Kumar, M.; Miravet, J. F.; Ulijn, R. V.; Escuder, B., Peptide-Based Molecular Hydrogels as Supramolecular Protein Mimics. *Chem. Eur. J.* **2017,** *23* (5), 981-993.
(7) Du, X.; Zhou, J.; Shi, J.; Xu, B., Supramolecular Hydrogelators and Hydrogels: From Soft Matter to Molecular Biomaterials. *Chem. Rev.* **2015,** *115* (24), 13165-307.
(8) Hanabusa, K.; Suzuki, M., Physical Gelation by Low-Molecular-Weight Compounds

and Development of Gelators. *Bull. Chem. Soc. Jpn.* **2016,** *89* (2), 174-182.
(9) Hendricks, M. P.; Sato, K.; Palmer, L. C.; Stupp, S. I., Supramolecular Assembly of Peptide Amphiphiles. *Acc. Chem. Res.* **2017,** *50* (10), 2440-2448.
(10) Wang, F.; Su, H.; Xu, D.; Dai, W.; Zhang, W.; Wang, Z.; Anderson, C. F.; Zheng, M.; Oh, R.; Wan, F.; Cui, H., Tumour sensitization via the extended intratumoural release of a STING agonist and camptothecin from a self-assembled hydrogel. *Nat. Biomed. Eng.* **2020**, 4(11),1090-1101.
(11) Sarkar, S.; Choudhury, P.; Dinda, S.; Das, P. K., Tailor-Made Self-Assemblies from Functionalized Amphiphiles: Diversity and Applications. *Langmuir* **2018,** *34* (36), 10449-10468.
(12) Scott, G. G.; McKnight, P. J.; Tuttle, T.; Ulijn, R. V., Tripeptide Emulsifiers. *Adv. Mater.* **2016,** *28* (7), 1381-13816.
(13) Nishida, Y.; Tanaka, A.; Yamamoto, S.; Tominaga, Y.; Kunikata, N.; Mizuhata, M.; Maruyama, T., In Situ Synthesis of a Supramolecular Hydrogelator at an Oil/Water Interface for Stabilization and Stimuli-Induced Fusion of Microdroplets. *Angew. Chem. Int. Ed.* **2017,** *56* (32), 9410-9414.
(14) He, H. J.; Xu, B., Instructed-Assembly (iA): A Molecular Process for Controlling Cell Fate. *Bull. Chem. Soc. Jpn.* **2018,** *91* (6), 900-906.
(15) Yang, Z. M.; Xu, K. M.; Guo, Z. F.; Guo, Z. H.; Xu, B., Intracellular Enzymatic Formation of Nanofibers Results in Hydrogelation and Regulated Cell Death. *Adv. Mater.* **2007,** *19* (20), 3152-3156.
(16) Yang, Z.; Liang, G.; Guo, Z.; Guo, Z.; Xu, B., Intracellular hydrogelation of small molecules inhibits bacterial growth. *Angew. Chem. Int. Ed.* **2007,** *46* (43), 8216-9.
(17) Vollenbroich, D.; Pauli, G.; Ozel, M.; Vater, J., Antimycoplasma properties and application in cell culture of surfactin, a lipopeptide antibiotic from Bacillus subtilis. *Appl. Environ. Microbiol.* **1997,** *63* (1), 44-49.
(18) Martinez, J. S.; Zhang, G. P.; Holt, P. D.; Jung, H. T.; Carrano, C. J.; Haygood, M. G.; Butler, A., Self-assembling amphiphilic siderophores from marine bacteria. *Science* **2000,** *287* (5456), 1245-1247.
(19) Mulligan, C. N., Environmental applications for biosurfactants. *Environ. Pollut.* **2005,** *133* (2), 183-198.
(20) Dong, Y. Z.; Love, K. T.; Dorkin, J. R.; Sirirungruang, S.; Zhang, Y. L.; Chen, D. L.; Bogorad, R. L.; Yin, H.; Chen, Y.; Vegas, A. J.; Alabi, C. A.; Sahay, G.; Olejnik, K. T.; Wang, W. H.; Schroeder, A.; Lytton-Jean, A. K. R.; Siegwart, D. J.; Akinc, A.; Barnes,

C.; Barros, S. A.; Carioto, M.; Fitzgerald, K.; Hettinger, J.; Kumar, V.; Novobrantseva, T. I.; Qin, J. N.; Querbes, W.; Koteliansky, V.; Langer, R.; Anderson, D. G., Lipopeptide nanoparticles for potent and selective siRNA delivery in rodents and nonhuman primates. *Proc. Natl. Acad. Sci. USA* **2014,** *111* (11), 3955-3960.
(21) He, H. J.; Guo, J. Q.; Lin, X. Y.; Xu, B., Enzyme-Instructed Assemblies Enable Mitochondria Localization of Histone H2B in Cancer Cells. *Angew. Chem. Int. Ed.* **2020,** *59* (24), 9330-9334.
(22) Tanaka, A.; Fukuoka, Y.; Morimoto, Y.; Honjo, T.; Koda, D.; Goto, M.; Maruyama, T., Cancer Cell Death Induced by the Intracellular Self-Assembly of an Enzyme-Responsive Supramolecular Gelator. *J. Am. Chem. Soc.* **2015,** *137*, 770-775.
(23) Pires, R. A.; Abul-Haija, Y. M.; Costa, D. S.; Novoa-Carballal, R.; Reis, R. L.; Ulijn, R. V.; Pashkuleva, I., Controlling Cancer Cell Fate Using Localized Biocatalytic Self-Assembly of an Aromatic Carbohydrate Amphiphile. *J. Am. Chem. Soc.* **2015,** *137* (2), 576-579.
(24) Jeena, M. T.; Palanikumar, L.; Go, E. M.; Kim, I.; Kang, M. G.; Lee, S.; Park, S.; Choi, H.; Kim, C.; Jin, S. M.; Bae, S. C.; Rhee, H. W.; Lee, E.; Kwak, S. K.; Ryu, J. H., Mitochondria localization induced self-assembly of peptide amphiphiles for cellular dysfunction. *Nat. Commun.* **2017,** *8* (1), 26.
(25) Zhan, J.; Cai, Y. B.; He, S. S.; Wang, L.; Yang, Z. M., Tandem Molecular Self-Assembly in Liver Cancer Cells. *Angew. Chem. Int. Ed.* **2018,** *57* (7), 1813-1816.
(26) Moore, L. L.; Bostick, D. A.; Garry, R. F., Sindbis virus infection decreases intracellular pH: alkaline medium inhibits processing of Sindbis virus polyproteins. *Virology* **1988,** *166* (1), 1-9.
(27) Gerweck, L. E.; Seetharaman, K., Cellular pH gradient in tumor versus normal tissue: potential exploitation for the treatment of cancer. *Cancer Res.* **1996,** *56* (6), 1194-8.
(28) Webb, B. A.; Chimenti, M.; Jacobson, M. P.; Barber, D. L., Dysregulated pH: a perfect storm for cancer progression. *Nat. Rev. Cancer* **2011,** *11* (9), 671-7.
(29) Kruk, J.; Aboul-Enein, H. Y., Reactive Oxygen and Nitrogen Species in Carcinogenesis: Implications of Oxidative Stress on the Progression and Development of Several Cancer Types. *Mini-Reviews in Medicinal Chemistry* **2017,** *17* (11), 904-919.
(30) Kwon, S.; Ko, H.; You, D. G.; Kataoka, K.; Park, J. H., Nanomedicines for Reactive Oxygen Species Mediated Approach: An Emerging Paradigm for Cancer Treatment. *Acc. Chem. Res.* **2019,** *52* (7), 1771-1782.

(31) Ciriolo, M. R.; Palamara, A. T.; Incerpi, S.; Lafavia, E.; Bue, M. C.; De Vito, P.; Garaci, E.; Rotilio, G., Loss of GSH, oxidative stress, and decrease of intracellular pH as sequential steps in viral infection. *J. Biol. Chem.* **1997,** *272* (5), 2700-8.
(32) Takahashi, S.; Kagami, Y.; Hanaoka, K.; Terai, T.; Komatsu, T.; Ueno, T.; Uchiyama, M.; Koyama-Honda, I.; Mizushima, N.; Taguchi, T.; Arai, H.; Nagano, T.; Urano, Y., Development of a Series of Practical Fluorescent Chemical Tools To Measure pH Values in Living Samples. *J. Am. Chem. Soc.* **2018,** *140* (18), 5925-5933.
(33) Cody, S. H.; Dubbin, P. N.; Beischer, A. D.; Duncan, N. D.; Hill, J. S.; Kaye, A. H.; Williams, D. A., Intracellular Ph Mapping with Snarf-1 and Confocal Microscopy .1. A Quantitative Technique for Living Tissues and Isolated Cells. *Micron* **1993,** *24* (6), 573-580.
(34) Rodriguez-Enriquez, S.; Gallardo-Perez, J. C.; Aviles-Salas, A.; Marin-Hernandez, A.; Carreno-Fuentes, L.; Maldonado-Lagunas, V.; Moreno-Sanchez, R., Energy metabolism transition in multi-cellular human tumor spheroids. *J. Cell. Physiol.* **2008,** *216* (1), 189-197.
(35) Hu, M.; Yang, Y.; Meng, C.; Pan, Z.; Jiao, X., Responses of macrophages against Salmonella infection compared with phagocytosis. *In Vitro Cell. Dev. Biol. Anim.* **2013,** *49* (10), 778-84.
(36) Sun, C. Y.; Shen, S.; Xu, C. F.; Li, H. J.; Liu, Y.; Cao, Z. T.; Yang, X. Z.; Xia, J. X.; Wang, J., Tumor Acidity-Sensitive Polymeric Vector for Active Targeted siRNA Delivery. *J. Am. Chem. Soc.* **2015,** *137* (48), 15217-24.
(37) Kanamala, M.; Wilson, W. R.; Yang, M. M.; Palmer, B. D.; Wu, Z. M., Mechanisms and biomaterials in pH-responsive tumour targeted drug delivery: A review. *Biomaterials* **2016,** *85*, 152-167.
(38) He, N.; Chen, Z.; Yuan, J.; Zhao, L.; Chen, M.; Wang, T.; Li, X., Tumor pH-Responsive Release of Drug-Conjugated Micelles from Fiber Fragments for Intratumoral Chemotherapy. *ACS Appl. Mater. Interfaces* **2017,** *9* (38), 32534-32544.
(39) Guo, X.; Wang, L.; Duval, K.; Fan, J.; Zhou, S.; Chen, Z., Dimeric Drug Polymeric Micelles with Acid-Active Tumor Targeting and FRET-Traceable Drug Release. *Adv. Mater.* **2018,** *30* (3), 1705436.
(40) Chan, Y.; Wong, T.; Byrne, F.; Kavallaris, M.; Bulmus, V., Acid-labile core cross-linked micelles for pH-triggered release of antitumor drugs. *Biomacromolecules* **2008,** *9* (7), 1826-1836.
(41) Fan, J. Q.; Zeng, F.; Wu, S. Z.; Wang, X. D., Polymer Micelle with pH-Triggered

Hydrophobic-Hydrophilic Transition and De-Cross-Linking Process in the Core and Its Application for Targeted Anticancer Drug Delivery. *Biomacromolecules* **2012,** *13* (12), 4126-4137.
(42) Yildirim, T.; Traeger, A.; Sungur, P.; Hoeppener, S.; Kellner, C.; Yildirim, I.; Pretzel, D.; Schubert, S.; Schubert, U. S., Polymersomes with Endosomal pH-Induced Vesicle-to-Micelle Morphology Transition and a Potential Application for Controlled Doxorubicin Delivery. *Biomacromolecules* **2017,** *18* (10), 3280-3290.
(43) Kuang, Y.; Miki, K.; Parr, C. J. C.; Hayashi, K.; Takei, I.; Li, J.; Iwasaki, M.; Nakagawa, M.; Yoshida, Y.; Saito, H., Efficient, Selective Removal of Human Pluripotent Stem Cells via Ecto-Alkaline Phosphatase-Mediated Aggregation of Synthetic Peptides. *Cell Chem. Biol.* **2017,** *24* (6), 685-694 e4.
(44) Koda, D.; Maruyama, T.; Minakuchi, N.; Nakashima, K.; Goto, M., Proteinase-mediated drastic morphological change of peptide-amphiphile to induce supramolecular hydrogelation. *Chem. Commun.* **2010,** *46* (6), 979-81.
(45) Lin, B. F.; Megley, K. A.; Viswanathan, N.; Krogstad, D. V.; Drews, L. B.; Kade, M. J.; Qian, Y. C.; Tirrell, M. V., pH-responsive branched peptide amphiphile hydrogel designed for applications in regenerative medicine with potential as injectable tissue scaffolds. *J. Mater. Chem.* **2012,** *22* (37), 19447-19454.
(46) Ray, S.; Das, A. K.; Banerjee, A., pH-responsive, bolaamphiphile-based smart metallo-hydrogels as potential dye-adsorbing agents, water purifier, and vitamin B-12 carrier. *Chem. Mater.* **2007,** *19* (7), 1633-1639.
(47) Shome, A.; Debnath, S.; Das, P. K., Head group modulated pH-responsive hydrogel of amino acid-based amphiphiles: Entrapment and release of cytochrome c and vitamin B-12. *Langmuir* **2008,** *24* (8), 4280-4288.
(48) Ghosh, A.; Haverick, M.; Stump, K.; Yang, X.; Tweedle, M. F.; Goldberger, J. E., Fine-tuning the pH trigger of self-assembly. *J. Am. Chem. Soc.* **2012,** *134* (8), 3647-50.
(49) Cote, Y.; Fu, I. W.; Dobson, E. T.; Goldberger, J. E.; Nguyen, H. D.; Shen, J. K., Mechanism of the pH-Controlled Self-Assembly of Nanofibers from Peptide Amphiphiles. *J. Phys. Chem. C* **2014,** *118* (29), 16272-16278.
(50) Minakuchi, N.; Hoe, K.; Yamaki, D.; Ten-No, S.; Nakashima, K.; Goto, M.; Mizuhata, M.; Maruyama, T., Versatile supramolecular gelators that can harden water, organic solvents and ionic liquids. *Langmuir* **2012,** *28* (25), 9259-66.
(51) Capito, R. M.; Azevedo, H. S.; Velichko, Y. S.; Mata, A.; Stupp, S. I., Self-assembly of large and small molecules into hierarchically ordered sacs and membranes. *Science*

2008, *319* (5871), 1812-1816.
(52) Mei, L. X.; He, S. Y.; Zhang, L.; Xu, K. M.; Zhong, W. Y., Supramolecular self-assembly of fluorescent peptide amphiphiles for accurate and reversible pH measurement. *Org. Biomol. Chem.* 2019, *17* (4), 939-944.
(53) Carey, M. C.; Small, D. M., Micellar properties of dihydroxy and trihydroxy bile salts: effects of counterion and temperature. *J. Colloid Interface Sci.* 1969, *31* (3), 382-96.
(54) Inoue, M.; Yamada, H.; Yasukochi, T.; Kuroki, R.; Miki, T.; Horiuchi, T.; Imoto, T., Multiple role of hydrophobicity of tryptophan-108 in chicken lysozyme: structural stability, saccharide binding ability, and abnormal pKa of glutamic acid-35. *Biochemistry* 1992, *31* (24), 5545-5553.
(55) Gao, Y.; Shi, J.; Yuan, D.; Xu, B., Imaging enzyme-triggered self-assembly of small molecules inside live cells. *Nat. Commun.* 2012, *3*, 1033.
(56) Fadok, V. A.; Voelker, D. R.; Campbell, P. A.; Cohen, J. J.; Bratton, D. L.; Henson, P. M., Exposure of Phosphatidylserine on the Surface of Apoptotic Lymphocytes Triggers Specific Recognition and Removal by Macrophages. *J. Immunol.* 1992, *148* (7), 2207-2216.
(57) Yoshida, H., ER stress and diseases. *FEBS J* 2007, *274* (3), 630-58.
(58) Kim, B. J.; Fang, Y.; He, H. J.; Xu, B., Trypsin-Instructed Self-Assembly on Endoplasmic Reticulum for Selectively Inhibiting Cancer Cells. *Adv. Healthc. Mater.* 2021, 10, 2000416.
(59) He, H. J.; Liu, S.; Wu, D. F.; Xu, B., Enzymatically Formed Peptide Assemblies Sequestrate Proteins and Relocate Inhibitors to Selectively Kill Cancer Cells. *Angew. Chem. Int. Ed.* 2020, *59* (38), 16445-16450.
(60) Wang, L. L.; Guan, R. L.; Xie, L. N.; Liao, X. X.; Xiong, K.; Rees, T. W.; Chen, Y.; Ji, L. N.; Chao, H., An ER-Targeting Iridium(III) Complex That Induces Immunogenic Cell Death in Non-Small-Cell Lung Cancer. *Angew. Chem. Int. Ed.* 2021, 60, 4657-4665.
(61) Roy, S.; Dasgupta, A.; Das, P. K., Alkyl chain length dependent hydrogelation of L-tryptophan-based amphiphile. *Langmuir* 2007, *23* (23), 11769-11776.
(62) Feng, Z. Q. Q.; Wang, H. M.; Chen, X. Y.; Xu, B., Self-Assembling Ability Determines the Activity of Enzyme-Instructed Self-Assembly for Inhibiting Cancer Cells. *J. Am. Chem. Soc.* 2017, *139* (43), 15377-15384.
(63) Ishida, M.; Watanabe, H.; Takigawa, K.; Kurishita, Y.; Oki, C.; Nakamura, A.;

Hamachi, I.; Tsukiji, S., Synthetic Self-Localizing Ligands That Control the Spatial Location of Proteins in Living Cells. *J. Am. Chem. Soc.* **2013,** *135* (34), 12684-12689.
(64) Kitaoka, M.; Imamura, K.; Hirakawa, Y.; Tahara, Y.; Kamiya, N.; Goto, M., Needle-free immunization using a solid-in-oil nanodispersion enhanced by a skin-permeable oligoarginine peptide. *Int. J. Pharm.* **2013,** *458* (2), 334-339.
(65) Wakabayashi, R.; Sakuragi, M.; Kozaka, S.; Tahara, Y.; Kamiya, N.; Goto, M., Solid-in-Oil Peptide Nanocarriers for Transcutaneous Cancer Vaccine Delivery against Melanoma. *Mol Pharm* **2018,** *15* (3), 955-961.

For Table of Contents Use Only

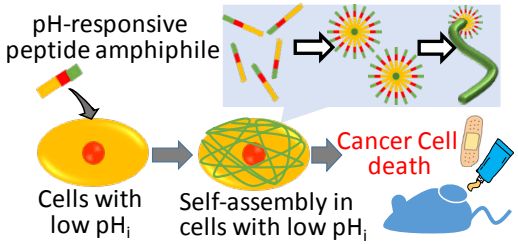

Microenvironment pH-induced selective cell death for potential cancer therapy using nanofibrous self-assembly of a peptide amphiphile

Shota Yamamoto, Kanon Nishimura, Kenta Morita, Sayuki Kanemitsu, Yuki Nishida, Tomoyuki Morimoto, Takashi Aoi, Atsuo Tamura and Tatsuo Maruyama

Supporting Information

Microenvironment pH-induced selective cell death for potential cancer therapy using nanofibrous self-assembly of a peptide amphiphile

Shota Yamamoto,[a] Kanon Nishimura, [a] Kenta Morita, [a] Sayuki Kanemitsu, [a] Yuki Nishida,[a] Tomoyuki Morimoto, [a] Takashi Aoi[b], Atsuo Tamura[c] and Tatsuo Maruyama[a, d]*

[a]Department of Chemical Science and Engineering, Graduate School of Engineering, Kobe University, 1-1 Rokkodai, Nada-ku, Kobe 657-8501, Japan.

[b]Division of Advanced Medical Science, Graduate School of Science, Technology and Innovation, Kobe University, Kobe 657-8501, Japan.

[c]Graduate School of Science, Department of Chemistry, Kobe University, Nada, Kobe 657-8501, Japan.

[d]Research Center for Membrane and Film Technology, Kobe University, 1-1 Rokkodai, Nada, Kobe 657-8501, Japan

KEYWORDS. antitumor, cytotoxicity, lipopeptide, nanofiber, pH-sensitive

Experimental

Materials

Fmoc amino acids, 12-(Fmoc-amino)dodecanoic acid (Fmoc-Adod(12)-OH), H-Glu(OtBu)-(Trt)-Trt(2-Cl)-resin,,1-hydroxybenzotriazole hydrate (HOBT·H_2O), 2-(1H-benzotriazole-1-yl)-1,1,3,3-tetramethyluronium hexafluorophosphate (HBTU), triisopropylsilane (TIPS) and *N*,*N*-dimethylformamide (DMF) were purchased from Watanabe Chemical Industry (Hiroshima, Japan). Trifluoroacetic acid (TFA), dichloromethane (DCM), methanol, palmitic acid, caprylic acid, capric acid, sodium hydroxide aqueous solution and hydrochloric acid were purchased from Fujifilm Wako Pure Chemical Co., Ltd. (Osaka, Japan). *N,N*-Diisopropylethylamine (DIEA), piperidine, 4-chloro-7-nitro-2,1,3-benzoxadiazole (NBD-Cl), 2,5-dihydroxybenzoic acid (DHB) and sinapinic acid (SA) were purchased from Tokyo Chemical Industry (Tokyo, Japan). Kaiser reagents for ninhydrin tests were purchased from Kokusan Chemical (Tokyo, Japan). High quality deionized water (DI water, > 15 MΩ·cm) produced by an Elix-5 system (Millipore, Molsheim, France) was used.

Results

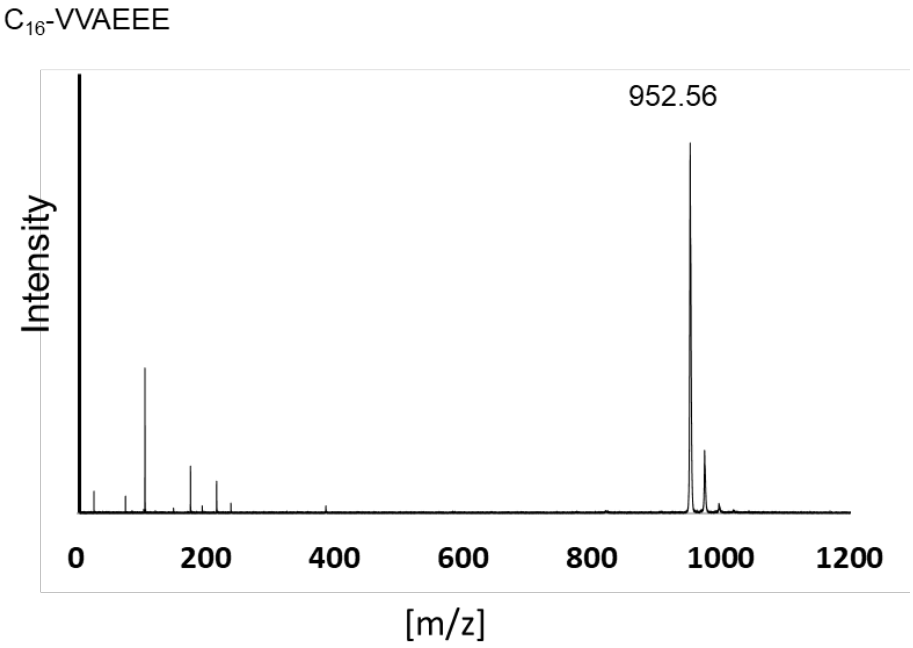

Figure S1. MALDI-TOF/MS spectrum of C_{16}-VVAEEE.

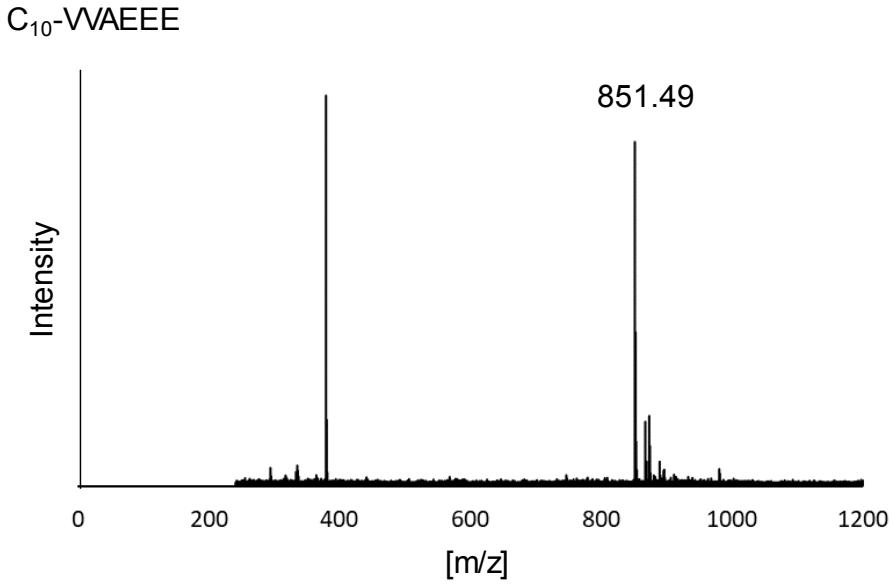

Figure S2. MALDI-TOF/MS spectrum of C_{10}-VVAEEE.

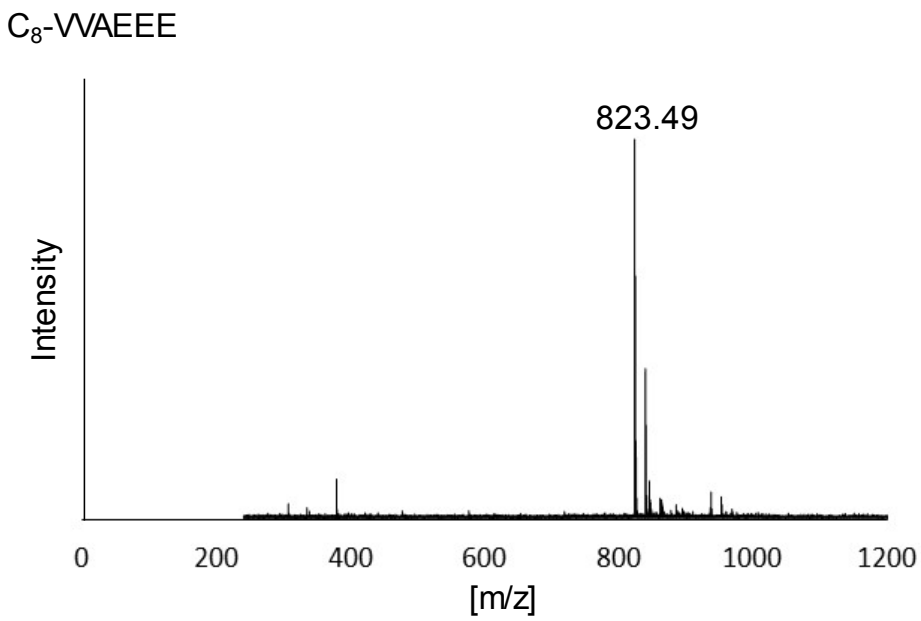

Figure S3. MALDI-TOF/MS spectrum of C_8-VVAEEE.

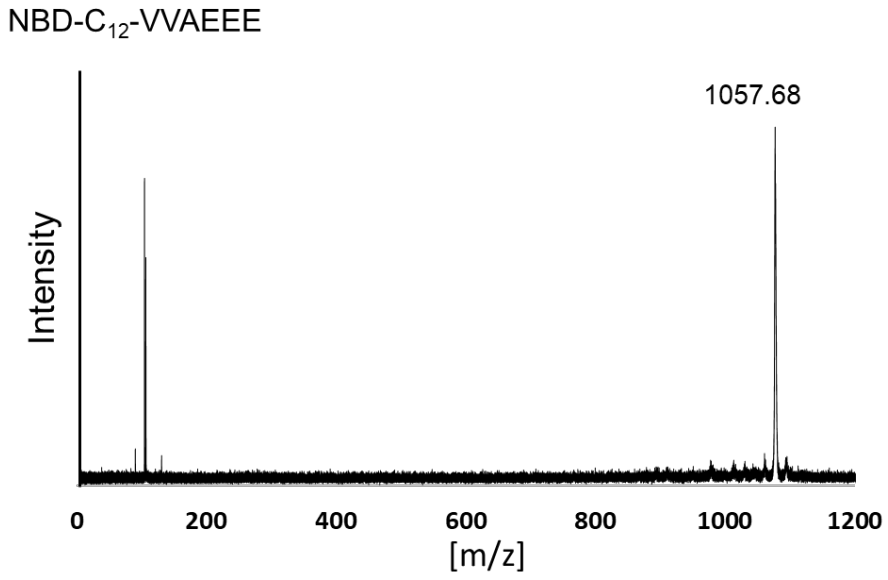

Figure S4. MALDI-TOF/MS spectrum of NBD-C_{12}-VVAEEE.

Results

Table S1. Gelation tests of various peptide amphiphiles using Dulbecco's phosphate-buffered saline.*

Sequence	pH 6.8	pH 7.0	pH 7.2	pH 7.4
C_{14}-VVAKE	VS	VS	VS	G
C_{14}-IIAKE	G	G	G	G
C_{14}-VVAKEE	S	S	G	G
C_{14}-VVAEE	VS	OS	OS	OS
C_{14}-VVADD	G	G	VS	S
C_{16}-VVAEEE	G	S	S	S
C_{14}-VVAEEE	S	S	S	S
C_{10}-VVAEEE	S	S	S	S
C_{8}-VVAEEE	S	S	S	S

*The concentration of the peptide amphiphiles was 0.15 wt%. Gelation was confirmed by the test-tube inverting method. G, gel; S, sol; VS, viscous solution; OS, opaque solution.

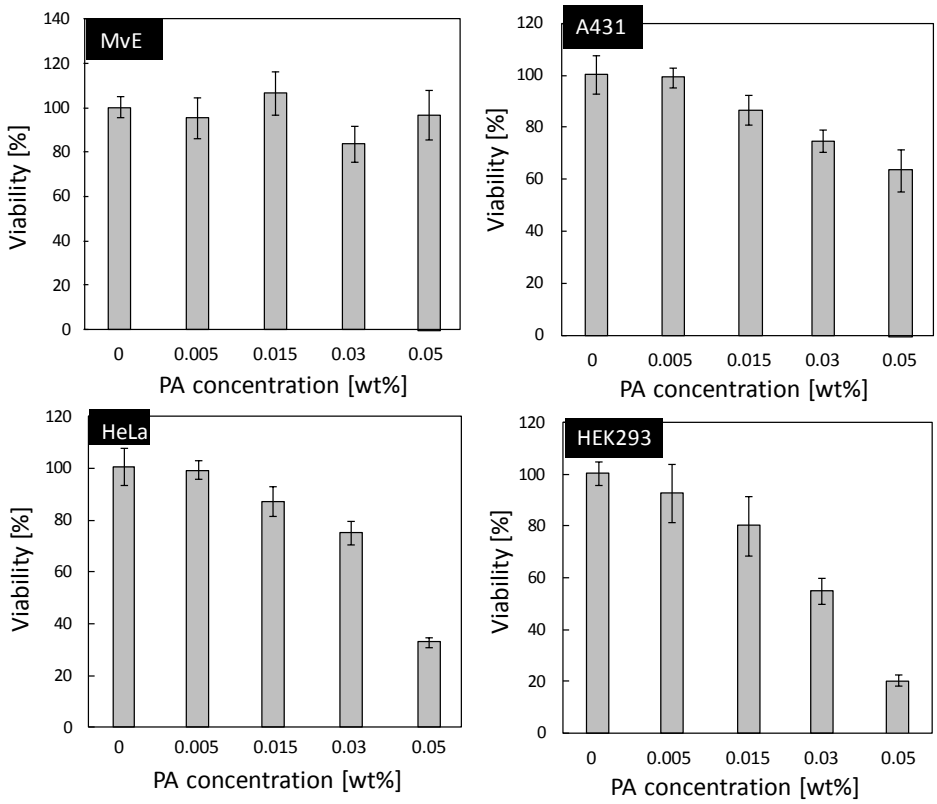

Figure S5. Effect of the PA (C_{16}-VVAEEE) concentration on the viability of the four different cell lines examined. Viability was assayed after 24 h incubation with C_{16}-VVAEEE.

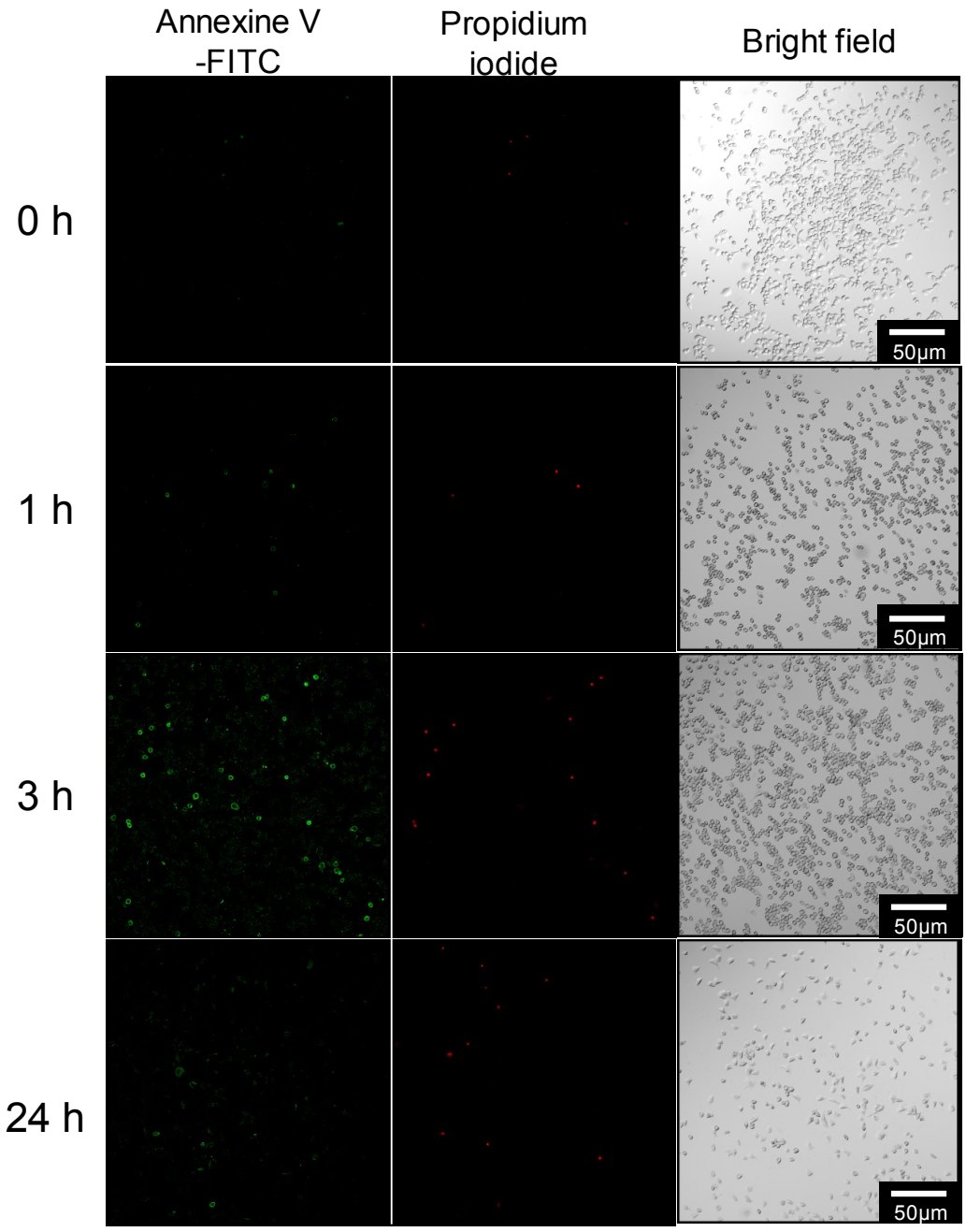

Figure S6. Apoptotic/necrotic assay. HeLa cells, which were treated with with C_{16}-VVAEEE (0.3wt%) for 24 h, were stained with FITC-annexin V and propidium iodide (PI).

Apoptotic/necrotic/healthy cells detection kit (Promo cell, GmbH, Heidelberg, Germany) was used to detect the apoptosis according to the manufacturer's protocols. Briefly, HeLa cells in a glass-base dish were washed with a binding buffer. A staining solution was added to microplate wells and cells were incubated for 15 min at 25 °C, followed by washing with a binding buffer. Cells were visualized using a CLSM.

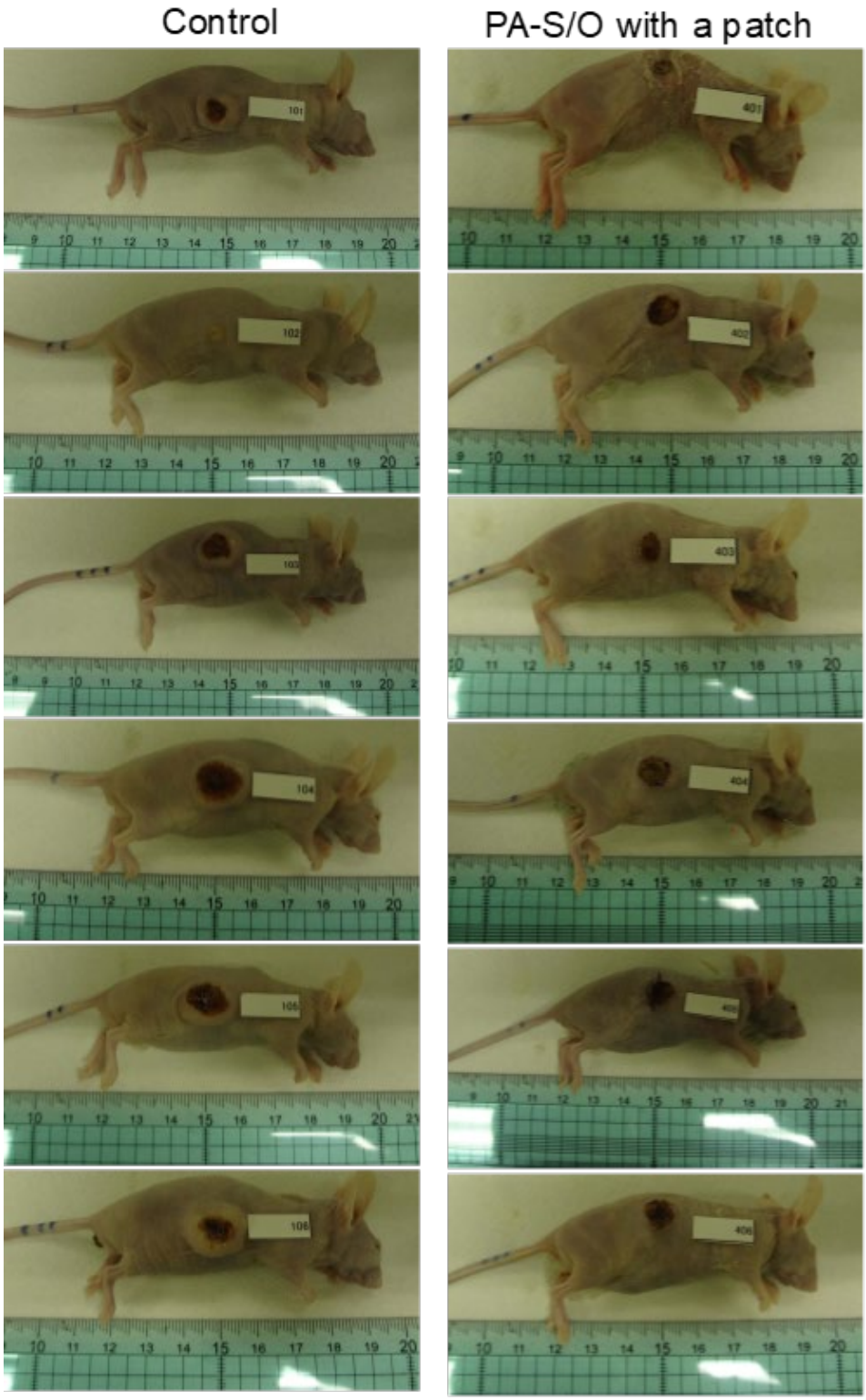

Figure S7. Photos of HeLa tumor-bearing mice after the transcutaneous administration of PA-S/O dispersion (with a patch) for 3 weeks.